Inorganic Chemistry

Article

pubs.acs.org/IC

Synthesis, Characterization, and Photophysical and Electroluminescent Properties of Blue-Emitting Cationic Iridium(III) Complexes Bearing Nonconjugated Ligands

Fuli Zhang,*[,†] Dongxin Ma,[‡] Lian Duan,*[,‡] Juan Qiao,[‡] Guifang Dong,[‡] Liduo Wang,[‡] and Yong Qiu[‡]

[†]College of Chemistry and Chemical Engineering, Shangqiu Normal University, Shangqiu 476000, P. R. China

[‡]Key Lab of Organic Optoelectronics and Molecular Engineering of Ministry of Education, Department of Chemistry, Tsinghua University, Beijing 100084, P. R. China

Supporting Information

ABSTRACT: The development of pure-blue-to-deep-blue-emitting ionic phosphors is an ultimate challenge for full-color displays and white-light sources. Herein we report two series of short-wavelength light-emitting cationic iridium(III) complexes with nonconjugated ancillary and cyclometalating ligands, respectively. In the first series, nonconjugated 1-[(diphenylphosphino)methyl]-3-methylimidazolin-2-ylidene-C,C_2' (dppmmi) is used as the ancillary ligand and 2-phenylpyridine (ppy), 2-(2,4-difluorophenyl)pyridine (dfppy), and 1-(2,4-difluorophenyl)-1*H*-pyrazole (dfppz) are used as cyclometalating ligands. In the second one, nonconjugated 2,4-difluorobenzyl-*N*-pyrazole (dfbpz) is used as the cyclometalating ligand and 3-methyl-1-(2-pyridyl)-benzimidazolin-2-ylidene-C,$C^{2'}$ (pymbi) as the ancillary ligand. The synthesis and photophysical and electrochemical properties, together with the X-ray crystal structures of these complexes, have been investigated. At room temperature, blue-emitting complexes $[Ir(ppy)_2(dppmmi)]PF_6$ (**1**) and $[Ir(dfppy)_2(dppmmi)]PF_6$ (**2**; PF_6^- is hexafluorophosphate) show much larger photoluminescence quantum yields of 24% and 46%, respectively. On the contrary, for complexes $[Ir(dfppz)_2(dppmmi)]PF_6$ (**3**) and $[Ir(dfbpz)_2(pymbi)]PF_6$ (**4**), deep-blue luminescence is only observed at low temperature (77 K). Density functional theory calculations are used to rationalize the differences in the photophysical behavior observed upon changes of the ligands. It is shown that the electronic transition dipoles of cationic iridium complexes **1** and **2** are mainly confined to cyclometalated ligands (^{3}MLCT and LC $^3\pi-\pi^*$) and those of complex **3** are confined to all of the ligands (^{3}MLCT, LC $^3\pi-\pi^*$, and ^{3}LLCT) because of the high LUMO energy level of dfppz. The emission of **4** mainly originates from the central iridium(III) ion and cyclometalated ligand to ancillary ligand charge transfer (^{3}MLCT and ^{3}LLCT), in contrast to commonly designed cationic complexes using carbene-type ancillary ligands, where emission originates from the cyclometalated main ligands. Solution-processed organic light-emitting diodes based on complexes **1** and **2** gave blue-green (498 nm) and blue (478 nm) electroluminescence with maximum current efficiencies of 3.8 and 3.4 cd A^{-1}, respectively. The results indicate that introducing nonconjugated ligands into cationic iridium complexes is an effective means of achieving short-wavelength light-emitting phosphors.

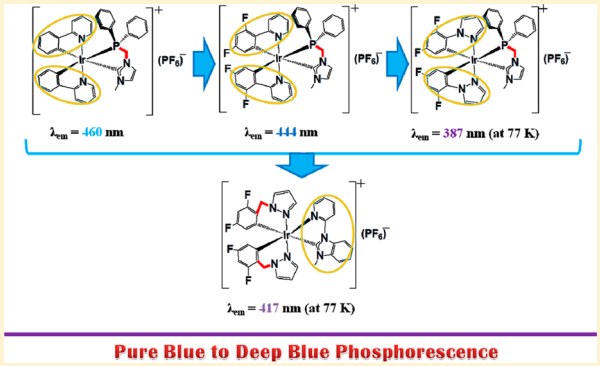

INTRODUCTION

Phosphorescent cationic iridium(III) complexes have exhibited enormous potential in organic electroluminescent (EL) devices, including light-emitting electrochemical cells[1−13] and organic light-emitting diodes (OLEDs),[14−21] because of their good solubilities, high photoluminescence quantum yields (PLQYs), and tunable light emission color. Most of the complexes reported in the literature typically emit in the red, orange, yellow, green, and sky-blue regions with high efficiencies. However, the development of pure-blue-to-deep-blue-emitting ionic phosphors is still an ultimate challenge for full-color displays and white-light sources.[22−24]

Experimental and theoretical studies have pointed out that, for traditional bpy-based (bpy is 2,2′-bipyridine) cationic iridium(III) complexes, the highest occupied molecular orbitals (HOMOs) reside on the iridium(III) ions and the phenyl rings of the cyclometalated ligands and the lowest unoccupied molecular orbitals (LUMOs) reside on the pyridine moieties of the ancillary ligands.[25] Two approaches have been adopted in order to obtain blue emission. One is to attach electron-withdrawing substitutents to the phenyl groups of the cyclometalated ligands[25−27] and the other is to attach electron-donating substitutents to the bpy-type ancillary ligands[28,29] to induce a large HOMO−LUMO energy gap. During the past few years, some blue-green-to-blue-emitting

Received: January 22, 2014
Published: June 10, 2014

   dx.doi.org/10.1021/ic5001733 | Inorg. Chem. 2014, 53, 6596−6606

cationic iridium(III) complexes have been reported with pyrazole,[7] imidazole,[8] and triazole[12,30] derivatives as ancillary ligands involving electron-donating nitrogen atoms, which lead to the destabilized LUMO and blue-shifted emission spectra of these complexes compared with those of $[Ir(ppy)_2(dtbbpy)]PF_6$ (ppy is 2-phenylpyridine, and dtbbpy is 4,4′-di-*tert*-butyl-2,2′-bipyridine).[1] An additional strategy to achieve efficient blue emission is to use a high-field-strength moiety such as N-heterocyclic carbene (NHC) as the ancillary ligand, which is a neutral two-electron donor and can destabilize the LUMO and metal-centered d−d excited states.[31] Ortí,[23,32] De Cola et al.[33] and our group[20] have developed a series of blue-to-near-UV-emitting cationic iridium(III) complexes based on NHCs.

In neutral iridium(III) complexes used in OLEDs, deep-blue emission has been achieved by using nonconjugated ligands containing methylene as the electronic blocker, the saturated nature of which could confine the electronic transition dipole around the 2-(2,4-difluorophenyl)pyridine (dfppy), 2-(4,6-difluorophenyl)-4-*tert*-butylpyridine (dfpbpy), 5-(2-pyridyl)-3-(trifluoromethyl)pyrazole (fppz), and 3-(trifluoromethyl)-5-(2-pyridyl)-1,2,4-triazole (fptz) chromophores.[34−37] Adopting this method, De Cola, Orti, and Baranoff developed deep-blue-emitting cationic bis-cyclometalated iridium(III) complexes with nonconjugated bis(imidazolium) carbene and bis-(pyrazole)-containing methylene as the ancillary ligand.[22,24,38] As anticipated, density functional theory (DFT) calculations based on these complexes show that the electronic transition dipole and emitting triplet state are mainly located on the cyclometalated chromophores.

The diphenylphosphine group (PPh_2) is a π acceptor, which can provide a much more stable five-membered metal−chelate bonding interaction with another coordination group, such as the benzyl moiety.[31] These kinds of ligands show a substantial increase of the ligand field strength and are capable of destabilizing the metal-centered d−d excited states concurrently. However, nonconjugated PPh_2-based ligands are generally used in neutral iridium(III) complexes.[35,36] Here, using nonconjugated 1-[(diphenylphosphino)methyl]-3-methylimidazolin-2-ylidene-C,C_2' (dppmmi) as the ancillary ligand and ppy, dfppy, and 1-(2,4-difluorophenyl)-1*H*-pyrazole (dfppz) as cyclometalated ligands, we report three cationic iridium(III) complexes, $[Ir(ppy)_2(dppmmi)]PF_6$ (**1**), $[Ir(dfppy)_2(dppmmi)]PF_6$ (**2**), and $[Ir(dfppz)_2(dppmmi)]PF_6$ (**3**). We propose that the ligand dppmmi bearing PPh_2 and imidazolium carbene moieties possesses higher ligand field strength and can further blue-shift emission spectra of these complexes. In addition, previously reported nonconjugated blue-emitting cationic iridium(III) complexes mainly use nonconjugated compounds as ancillary ligands, and corresponding complexes bearing nonconjugated cyclometalated ligands have not been reported. As a comparison to complexes **1**−**3**, using nonconjugated compound 2,4-difluorobenzyl-*N*-pyrazole (dfbpz) as the cyclometalated ligand, we prepared complex $[Ir(dfbpz)_2(pymbi)]PF_6$ (**4**) [pymbi is 3-methyl-1-(2-pyridyl)benzimidazolin-2-ylidene-C,$C^{2'}$]. Consequently, pure-blue to deep-blue phosphorescences of complexes **1**−**4** mainly from conjugated chromophoric ligands can easily be achieved through a facile synthetic approach elaborated as follows. Full photophysical and electrochemical characterizations have been performed, and the experimental results have been rationalized with quantum-chemical calculations. Solution-processed OLEDs based on complexes **1** and **2** gave blue-green (498 nm) and blue (478 nm) electroluminescence with maximum current efficiencies of 3.8 and 3.4 cd A^{-1}, respectively.

EXPERIMENTAL SECTION

Synthesis and Characterization. *General Procedures.* All reactants and solvents were used as received and were purified or dried by standard methods when required. All reactions were monitored using precoated thin-layer-chromatography plates (0.20 mm with fluorescent indicator UV254). ^1H NMR spectra were recorded on a JEOL JNMECA600 NMR spectrometer with tetramethylsilane $[Si(CH_3)_4]$ as the internal standard. Mass spectrometry (MS) was performed with an Esquire-LC_00136 mass spectrometer. Elemental analysis for carbon, hydrogen, and nitrogen was determined on an Exeter Analytical CE-440 elemental analyzer. The proligands $dppmmi^+Br^-$ and $pymbi^+I^-$ were prepared using literature procedures.[39,40] The dimeric iridium(III) intermediates $[(ppy)_2Ir(\mu\text{-}Cl)]_2$ and $[(dfppy)_2Ir(\mu\text{-}Cl)]_2$[41] and cyclometalated ligands dfppz[25] and dfbpz[34] were prepared according to the literature procedure.

Synthesis of $[Ir(ppy)_2(dppmmi)]PF_6$ (1). A mixture of $dppmmi^+Br^-$ (0.76 g, 2.11 mmol), Ag_2O (0.93 g, 4 mmol), and the dichloro-bridged cyclometalated iridium(III) complex $[(ppy)_2Ir(\mu\text{-}Cl)]_2$ (1.07 g, 1 mmol) in 2-ethoxyethanol (30 mL) was heated to reflux for 12 h under nitrogen in the dark. After cooling to room temperature, the solution was filtered through a sintered-glass frit, and an excess (10 equiv) of NH_4PF_6 (in 100 mL of H_2O) was added to induce precipitation. The yellow precipitate was collected by filtration, washed with excess H_2O, and then dried under vacuum. The crude product was purified by column chromatography on silica gel (200−300 mesh) with CH_2Cl_2 as the eluent. The product was then recrystallized from dichloromethane/hexane, yielding a light-yellow powder (0.45 g, 0.49 mmol). Yield: 25%. ^1H NMR (600 MHz, acetone-d_6, δ): 8.74 (d, J = 5.5 Hz, 1H), 8.24 (d, J = 8.3 Hz, 1H), 7.97 (t, J = 7.6 and 8.3 Hz, 1H), 7.88−7.92 (m, 2H), 7.76−7.83 (m, 4H), 7.72 (d, J = 6.2 Hz, 1H), 7.69 (t, J = 7.6 and 8.3 Hz, 1H), 7.58−7.61 (t, 1H), 7.45−7.47 (m, 2H), 7.27 (s, 1H), 7.13 (t, J = 7.6 Hz, 1H), 6.98−7.02 (m, 6H), 6.82 (t, J = 7.6 Hz, 1H), 6.72 (t, J = 7.6 Hz, 1H), 6.61−6.67 (m, 3H), 6.22 (m, 1H), 5.91 (m, 1H), 5.40 (d, J = 15.1 Hz, 1H), 3.11 (s, 3H). ESI-MS [m/z]: 781.2 $(M - PF_6)^+$. Anal. Found: C, 50.49; H, 3.70; N, 5.74. Anal. Calcd for $C_{39}H_{33}N_4P_2F_6Ir$: C, 50.59; H, 3.59; N, 6.05.

Synthesis of $[Ir(dfppy)_2(dppmmi)]PF_6$ (2). The synthesis of complex **2** is similar to that of complex **1**, except that ppy was replaced with dfppy. Yield: 75%. ^1H NMR (600 MHz, acetone-d_6, δ): 8.79 (d, J = 6.2 Hz, 1H), 8.44 (d, J = 9.6 Hz, 1H), 8.04−8.08 (m, 2H), 7.84−7.88 (m, 2H), 7.72−7.80 (m, 3H), 7.64 (t, J = 7.6 and 8.3 Hz, 1H), 7.52−7.54 (m, 2H), 7.36 (s, 1H), 7.18 (t, J = 7.6 Hz, 1H), 7.04−7.12 (m, 3H), 6.83 (t, J = 7.6 Hz, 1H), 6.10−6.73 (m, 4H), 6.10 (d, J = 6.2 Hz, 1H), 5.94−5.98 (m, 1H), 5.66−5.70 (m, 1H), 5.54 (d, J = 15.1 Hz, 1H), 3.24 (s, 3H). ESI-MS [m/z]: 853.2 $(M - PF_6)^+$. Anal. Found: C, 46.54; H, 2.88; N, 5.48. Anal. Calcd for $C_{39}H_{29}N_2P_2F_{10}Ir$: C, 46.94; H, 2.93; N, 5.61.

Synthesis of $[Ir(dfppz)_2(dppmmi)]PF_6$ (3). A mixture of dfppz (0.64 g, 3.58 mmol) and $IrCl_3{\cdot}3H_2O$ (0.60 g, 1.70 mmol) in 2-methoxyethanol (20 mL) was refluxed for 24 h under nitrogen in the dark. After the solution was cooled to room temperature, $dppmmi^+Br^-$ (0.62 g, 1.71 mmol) and Ag_2O (0.80 g, 3.61 mmol) were added, and the mixture was heated to reflux for a further 12 h under nitrogen in the dark. After cooling to room temperature, the solution was filtered through a sintered-glass frit, and an excess (10 equiv) of NH_4PF_6 (in 100 mL of H_2O) was added to induce precipitation. The yellow precipitate was collected by filtration, washed with excess H_2O, and then dried under vacuum. The crude product was purified by column chromatography on silica gel (200−300 mesh) with CH_2Cl_2/acetone (100:1) as the eluent. The product was then recrystallized from dichloromethane/acetone/hexane, yielding a light-yellow powder (1.27 g, 1.30 mmol). Yield: 76%. ^1H NMR (600 MHz, acetone-d_6, δ): 8.58 (s, 1H), 8.26 (s, 1H), 7.88 (s, 1H), 7.81 (m, 2H), 7.67 (m, 1H), 7.57 (m, 3H), 7.38 (s, 1H), 7.28 (m, 1H), 7.18 (m, 3H), 6.82 (m,

dx.doi.org/10.1021/ic5001733 | Inorg. Chem. 2014, 53, 6596−6606

Scheme 1. Synthetic Pathways and Structures of dppmmi$^+$Br$^-$ and Complexes 1−4

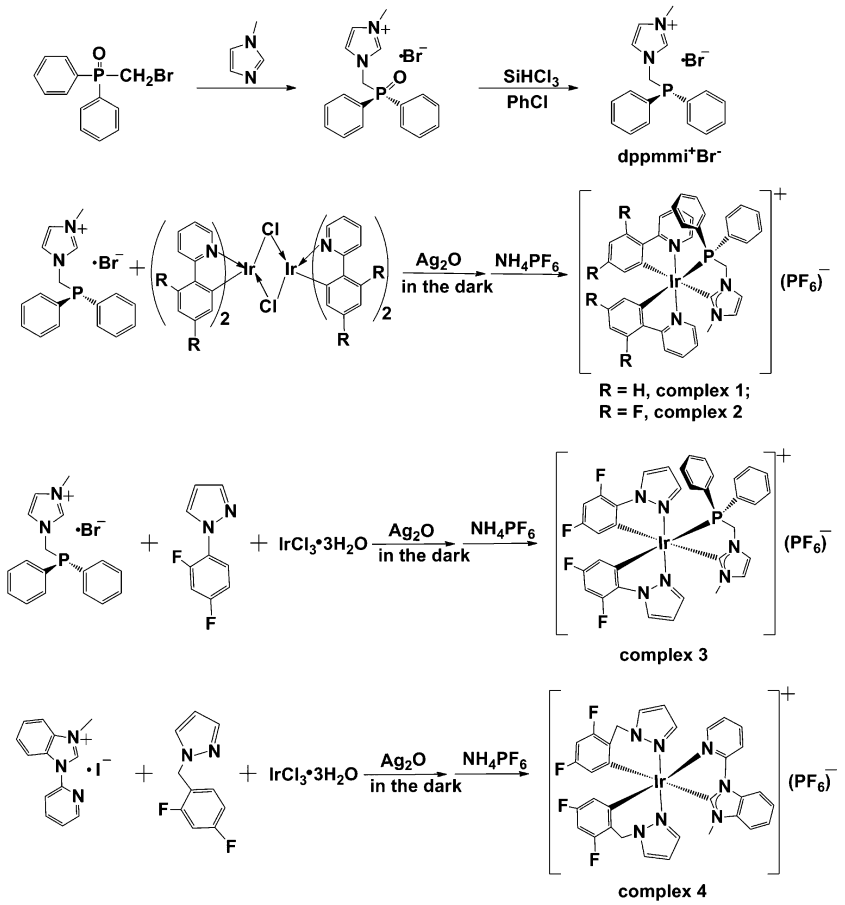

4H), 6.70 (s, 1H), 6.33 (s, 1H), 6.10 (d, J = 7.6 Hz, 1H), 5.96 (m, 1H), 5.72 (m, 1H), 5.38 (d, J = 15.1 Hz, 1H), 3.30 (s, 3H). ESI-MS [m/z]: 831.2 (M − PF_6)$^+$. Anal. Found: C, 42.94; H, 2.68; N, 8.47. Anal. Calcd for $C_{35}H_{27}N_6P_2F_{10}Ir$: C, 43.08; H, 2.79; N, 8.61.

Synthesis of [Ir(dfbpz)$_2$(pymbi)]PF$_6$ (4). The synthesis of complex **4** is similar to that of complex **3**, except that dfppz and dppmmi$^+$Br$^-$ were replaced with dfbpz and pymbi$^+$I$^-$, respectively. Yield: 24%. ^{1}H NMR (600 MHz, acetone-d_6, δ): 8.85 (d, J = 8.2 Hz, 1H), 8.54 (d, J = 8.3 Hz, 1H), 8.51 (d, J = 4.8 Hz,1H), 8.44 (m, 1H), 8.23 (s, 1H), 8.19 (s, 1H), 7.84 (d, J = 8.3 Hz, 1H), 7.65 (m, 3H), 7.39 (s, 1H), 7.12 (s, 1H), 6.66 (m, 2H), 6.34 (m, 2H), 5.93 (d, J = 8.9 Hz, 1H), 5.83 (d, J = 8.3 Hz, 1H), 5.48 (m, 2H), 5.20 (d, J = 15.1 Hz, 2H), 3.73 (s, 3H). ESI-MS [m/z]: 788.2 (M − PF_6)$^+$. Anal. Found: C, 42.43; H, 2.64; N, 10.31. Anal. Calcd for $C_{33}H_{25}N_7PF_{10}Ir$: C, 42.49; H, 2.70; N, 10.51.

Physical Measurements and Instrumentation. UV−vis absorption spectra were obtained from CH_3CN solutions and recorded with a UV−vis spectrophotometer (Agilent 8453). Steady-state emission spectra were recorded with a fluorospectrophotometer (Jobin Yvon, FluoroMax-3). Excited-state lifetimes were recorded at excitation wavelengths of 390 nm (for **1** and **2**) and 365 nm (for **3** and **4**) on a transient spectrofluorimeter (Edinburgh Instruments, FLSP920) with a time-correlated single-photon-counting technique. PLQYs for solution samples were measured by the optical dilute method with a degassed aqueous solution of quinine sulfate (PLQYs = 0.545 in 1 M H_2SO_4) as in ref 42. The solutions were degassed by three freeze−pump−thaw cycles before measurements. The thin films for testing of the photophysical properties were spin-coated onto the quartz glass in air and baked at 200 °C for 10 min. PLQYs in the thin films were measured with an integrating sphere in a fluorospectrophotometer (Jobin Yvon, FluoroMax-3) according to a reported procedure.[43] Cyclic voltammetry (CV) measurements were performed on a Princeton Applied Research potentiostat/galvanostat model 283 voltammetric analyzer in CH_3CN solutions (2×10^{-3} M) at a scan rate of 100 mV s^{-1}, with a platinum plate as the working electrode, a silver wire as the reference electrode, and a platinum wire as the counter electrode. The supporting electrolyte was tetrabutylammonium hexafluorophosphate ($TBAPF_6$; 0.1 M), and ferrocene (Fc) was used as the internal standard. All solutions for electrochemical studies were deaerated with prepurified argon gas just before measurements.

Crystal Structure Determination. The room temperature single-crystal X-ray experiments were performed on a Rigaku Saturn 724 + CCD diffractometer equipped with a graphite-monochromatized Mo Kα radiation. The structures were solved by direct methods and refined with a full-matrix least-squares technique based on F^2 with the *SHELXL-97* crystallographic software package.[44] All hydrogen atoms were generated theoretically and rode on their parent atoms in the final refinement.

Theoretical Calculations. DFT and time-dependent DFT (TD-DFT) at the spin-restricted B3LYP level were adopted for calculations on the ground and excited electronic states of the complexes.[45,46] "Double-ζ"-quality basis sets were employed for carbon, hydrogen, nitrogen, fluorine, and phosphorus (6-31G**)[47] and iridium (LANL2DZ).[48] An effective core potential replaces the inner-core electrons of iridium, leaving the outer core $5s^25p^6$ electrons and the $5d^6$ valence electrons of iridium(III).[48] All of the calculations were performed without applying any symmetry constraint and carried out with the *Gaussian 03* software package.[49]

Fabrication and Characterization of OLEDs. Indium−tin oxide (ITO) substrates with a sheet resistance of 15 Ω/□ were sufficiently cleaned using chemical and UV-ozone methods before deposition of the organic layers. The poly(3,4-ethylenedioxythiophene:poly-(styrenesulfonate) (PEDOT:PSS) layer was spin-coated onto the ITO substrate in air and baked at 200 °C for 10 min. The light-emitting layer was then spin-coated onto the PEDOT:PSS-coated substrate from a mixed solution of poly(*N*-vinylcarbazole) (PVK)/1,3-

dx.doi.org/10.1021/ic5001733 | *Inorg. Chem.* 2014, 53, 6596−6606

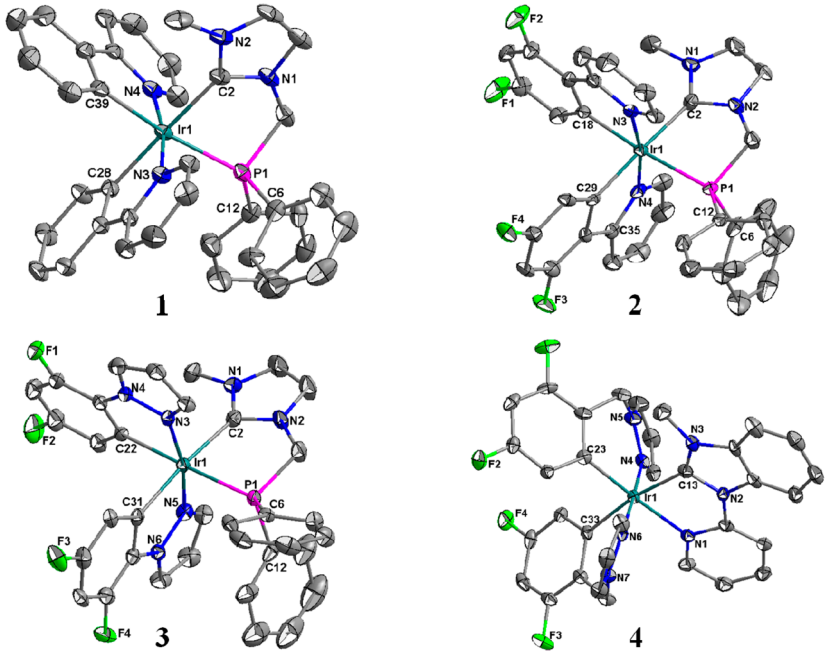

Figure 1. Crystal structures of complexes **1**–**4**. Counteranions PF_6^-, solvent molecules, and hydrogen atoms have been omitted for clarity. Thermal ellipsoids are drawn at 50% probability.

Table 1. Selected Bond Distances (Å) and Angles (deg) for Complexes 1–4

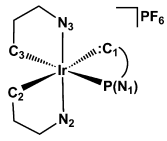

	1	2	3	4
		Distances		
Ir–C_1	2.1254(44)	2.1143(51)	2.1077(37)	2.0912(47)
Ir–$P(N_1)$	2.3484(12)	2.3567(11)	2.3380(13)	2.1593(40)
Ir–N_2	2.0548(34)	2.0593(29)	2.0190(39)	2.0567(34)
Ir–C_2	2.0599(37)	2.0455(51)	2.0750(37)	2.0874(47)
Ir–C_3	2.0503(37)	2.0509(40)	2.0647(41)	2.0387(43)
Ir–N_3	2.0776(38)	2.0685(26)	2.0359(38)	2.0580(34)
		Angles		
C_1–Ir–$P(N_1)$	78.031(146)	79.278(119)	79.732(107)	76.422(155)
C_1–Ir–C_2	177.098(158)	176.663(164)	172.974(142)	170.132(178)
C_1–Ir–C_3	95.463(175)	95.990(157)	98.913(144)	102.595(175)
$P(N_1)$–Ir–C_2	101.074(106)	99.311(123)	96.636(110)	95.526(154)
$P(N_1)$–Ir–C_3	172.918(108)	175.138(122)	178.489(113)	176.551(164)
C_2–Ir–C_3	85.560(149)	85.474(161)	84.782(147)	85.771(177)
N_2–Ir–N_3	170.369(134)	170.103(137)	169.336(164)	176.936(130)

bis[5-(4-*tert*-butylphenyl)-1,3,4-oxadiazol-2-yl]benzene (OXD-7)/complex **1** (or complex **2**) in 1,2-dichloroethane in a nitrogen-atmosphere glovebox and baked at 80 °C for 30 min. The substrate was then transferred into an evaporation chamber, where 1,3,5-tris(*N*-phenylbenzimidazole)benzene (TPBI) was evaporated at an evaporation rate of 1–2 Å s^{-1} under a pressure of 4×10^{-4} Pa and the Cs_2CO_3/Al bilayer cathode was evaporated at evaporation rates of 0.2 and 8–10 Å s^{-1} for Cs_2CO_3 and Al, respectively, under a pressure of 1×10^{-3} Pa. The current–voltage–brightness characteristics of the devices were recorded with a Keithley 4200 semiconductor characterization system. The EL spectra were collected with a Photo Research PR705 spectrophotometer. All measurements of the devices were carried out in an ambient atmosphere without further encapsulation.

RESULTS AND DISCUSSION

Synthesis and Characterization. Scheme 1 depicts the synthetic routes toward the ancillary proligand dppmmi$^+Br^-$ and complexes **1**–**4**. Ligand dppmmi$^+Br^-$ was directly synthesized from $Ph_2P(O)CH_2Br$[39] and 1-methylimidazole, followed by a reduction reaction with trichlorosilane (see the Supporting Information, SI). There are several purposes for using nonconjugated (P^C:) chelate dppmmi as the ancillary ligand. One is to inhibit π-orbital participation of the (P^C:) chelate at both HOMOs and LUMOs of the resulting iridium(III) complexes. Accordingly, color-tunable phosphorescences can be achieved through a simple switch of the chromophoric cyclometalated ligands with a much larger

dx.doi.org/10.1021/ic5001733 | Inorg. Chem. 2014, 53, 6596–6606

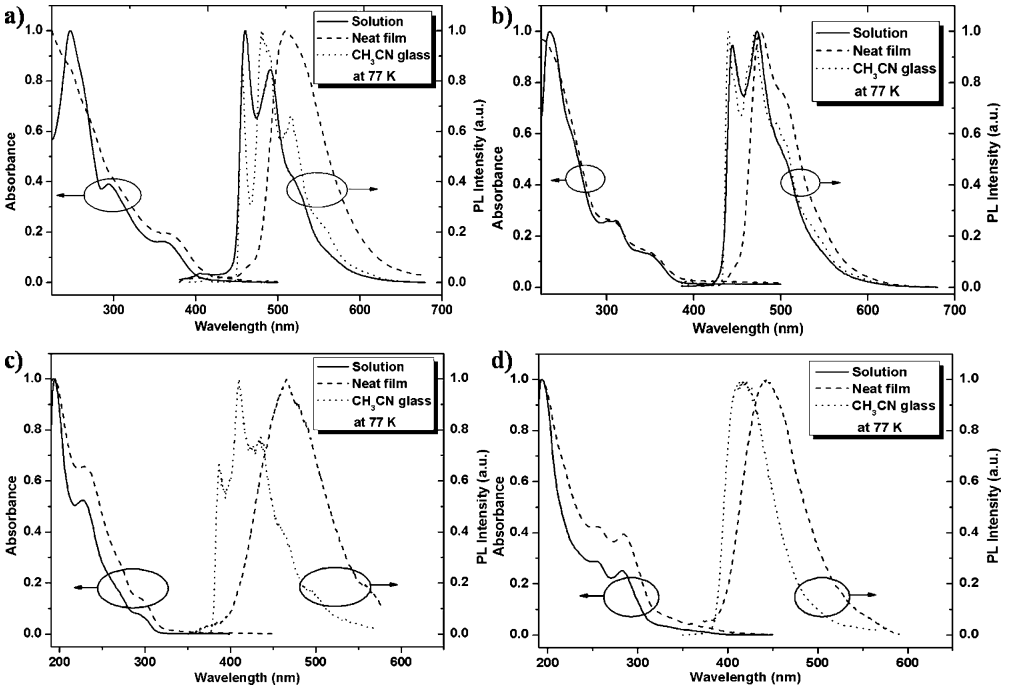

Figure 2. Absorption and PL spectra of (a) complex **1**, (b) complex **2**, (c) complex **3**, and (d) complex **4** in a CH_3CN solution and as neat films.

energy gap (cf. both dfppy and dfppz).[31,36] Also, the greater ligand field strength of the phosphine and carbene moieties could destabilize the metal-centered d−d excited states, which could become thermally inaccessible from the typical emissive triplet excited state. To test the concept that the short-wavelength phosphorescence of cationic iridium complexes can also be drastically tuned by using nonconjugated cyclometalated ligands, we synthesized a complex bearing cyclometalated ligand pymbi.

Complexes **1** and **2** were readily synthesized from the dimeric iridium(III) intermediate $[Ir(ppy)_2Cl]_2$ (or $[Ir(dfppy)_2Cl]_2$) and the ancillary ligand dppmmi$^+$Br$^-$ by a conventional synthetic method.[20,22] Complexes **3** and **4** were prepared by heating a 2:1 mixture of cyclometalated ligands and $IrCl_3{\cdot}3H_2O$ in 2-methoxyethanol (125 °C, 24 h), followed by the addition of 1 equiv of ancillary ligand in the presence of silver(I) oxide as the catalyst (125 °C, 12 h).[34] These complexes were fully structurally characterized by ^{1}H NMR (Figures S2−S5 in the SI), ESI (electrospray ionization)-MS (Figure S6 in the SI), and elemental analysis. Single-crystal X-ray diffraction studies on complexes **1**−**4** were carried out to reveal their exact formula and geometrical arrangement.

Single-Crystal Structures. Single crystals of complexes **1**−**4** were grown from slow evaporation of their methanol/acetone (1:1) solutions. The structures of complexes **1**−**4** are depicted in Figure 1, and selected bond lengths and angles are presented in Table 1. Similar to other cationic iridium(III) complexes,[7,20,25] complexes **1**−**4** exhibit distorted octahedral geometries around the iridium(III) centers, with two cyclometalated ligands adopting C,C-cis,N,N-trans configurations.

The bond distances and angles in **1**−**4** are almost equal to those in previously reported iridium(III) complexes.[7,20,22,25] It is worthnoting that, in complexes **1**−**3**, the Ir−C_2 (C_2 is the coordinated carbon trans to the carbene of the ancillary ligand) and Ir−C_3 (C_3 is the coordinated carbon trans to the phosphorus atom of the ancillary ligand) bonds are longer than the Ir−C bond trans to the pyridyl groups in previously reported iridium(III) complexes.[7,25] This phenomenon, in which the Ir−C_2 bond [2.0874(47) Å] is longer than the Ir−C_3 bond [2.0387(43) Å], can also be observed distinctly in complex **4**. It reflects the stronger trans effect of the carbene and phosphorus atom compared to the pyridine.

In complexes **1**−**3**, the metallacycle of the nonconjugated chelate dppmmi is slightly puckered, with the middle methylene being deviated from extension of the Ir−P−C_1 plane by 0.8260, 0.6810, and 0.4724 Å, respectively, because of the geometrical restriction imposed by both sp^3-hybridized phosphorus and methylene linkages.[36] In complex **4**, moreover, two middle methylenes of the nonconjugated cyclometalated dfbpz ligands exhibit significant deviation from extension of the Ir−N_2−C_2 and Ir−N_3−C_3 planes by 1.3726 and 1.3644 Å, respectively, because of the greater distortion of the six-membered chelate plane than of the five-membered chelate plane. Interestingly, except for complex **4**, the phenyl rings (Ph_{C6}, Ph_{C6}, and Ph_{C12} for complexes **1**−**3**, respectively) of the diphenylphosphino group exhibit intramolecular stacking interactions with the nitrogen heterocyclic rings (Het_{N3}, Het_{N4}, and Het_{N5} for complexes **1**−**3**, respectively) of the cyclometalated ligand, as shown in Figure 1. In complex **1**, the centroid−centroid distance and angle between the stacking rings are 3.9220(8) Å and 26.229(149)°. However, in complexes **2** and **3**, the stacking rings exhibit relatively small centroid−centroid distances [3.6522(6) and 3.4737(9) Å for **2** and **3**, respectively] and dihedral angles [17.296(170) and 20.674(195)° for **2** and **3**, respectively], which closely resemble those of other cationic iridium(III) complexes.[11,50,51] This suggests that substitution of the phenyl ring with two fluorine atoms can change the quadrupole moment of the nitrogen heterocyclic ring of the cyclometalated ligand to some extent and reinforce the intramolecular stacking interaction.

Photophysical Properties. The absorption and photoluminescent (PL) spectra of complexes **1**−**4** in a dilute CH_3CN solution and thin film are shown in Figure 2, and detailed photophysical characterizations are summarized in Table 2. The

dx.doi.org/10.1021/ic5001733 | Inorg. Chem. 2014, 53, 6596−6606

Table 2. Photophysical Characteristics of Complexes 1−4

		emission at room temperature					emission at 77 K[a]	
				Φ_{em} [τ [μs]]				
	absorption λ [nm] (ε [$\times 10^4$ M^{-1} cm^{-1}])[b]	solution λ [nm][c]	neat film λ [nm][d]	CH_3CN[c]	5 wt % in PMMA[e]	neat film[e]	λ [nm]	τ [μs][e]
1	247 (4.17)	460	516	0.24 [3.30]	0.59 [5.36 (91%), 1.12 (9%)]	0.05 [1.09 (36%) 0.51 (64%)]	457 sh	9.61
	293 (1.63)	491 sh					480	
	363 (0.67)						516 sh	
2	233 (6.36)	444 sh	476	0.46 [6.30]	0.66 [6.9(92%), 1.4 (8%)]	0.37 [1.6(15%) 0.8(85%)]	440	11.21
	311 (1.60)	473					470	
	353 (0.70)						495 sh	
3	227 (11.2)		465				387 sh	[38 (30%), 112 (70%)]
	293 (1.63)			[8.5]	[3.7 (96%), 0.04 (9%)]		410	
	332 (0.08)						435 sh	
4	254 (3.32)		442				417	[8 (91%), 60 (9%)]
	283 (2.81)			[5.7]	[4.7 (95%), 0.08 (5%)]			
	368 (0.16)							

[a]In CH_3CN glass at 77 K. [b]In CH_3CN solutions (1×10^{-5} M). [c]In degassed CH_3CN solutions; the symbol sh denotes the shoulder wavelength. [d]Neat films were made on quartz substrates with a thickness of about 100 nm. [e]The percentage in parentheses denotes the percentage of each lifetime.

strong absorption bands in the UV region (below about 340 nm for **1** and **2** and below about 275 nm for **3** and **4**, respectively) are attributed to spin-allowed $^1\pi-\pi^*$ transitions of the ligands and the relatively weak absorption bands extending to the visible region assigned to excitations to ^{1}MLCT (metal-to-ligand charge-transfer), ^{1}LLCT (ligand-to-ligand charge-transfer), ^{3}MLCT, ^{3}LLCT, and ligand-centered (LC) $^3\pi-\pi^*$ transitions.[7,8,12,22,52]

As depicted in Figure 2, complexes **1** and **2** show blue emission (peaks at 460 and 444 nm, respectively) in a CH_3CN solution at room temperature. Complex **2** exhibits a significant blue shift with respect to the corresponding dfppy-based cationic iridium(III) complex (λ_{em} = 452 nm) with non-conjugated bis(imidazolium) carbene as the ancillary ligand[22] because of the π-acceptor PPh_2 used. Complexes **3** and **4** are nonemitting at room temperature, as has been observed for iridium(III) complexes based on *N*-phenylpyrazole and NHC derivatives.[23,53,54] Nonradiative deactivation pathways involving a thermally accessible LLCT transition[55] (see the Theoretical Calculations section) or a high-lying metal-centered d−d transition[23,53,54] may be responsible for this phenomenon. When cooled to 77 K, **1** and **2** exhibit much more structured emission spectra with little rigidochromic blue shift of the 0−0 transition compared to their emission spectra at room temperature. This indicates that the emissive excited states of complexes **1** and **2** have strong LC $^3\pi-\pi^*$ character.[25,26,56,57] Notably, **3** and **4** have the highest energy emission in the deep-blue-region maxima at 387 and 417 nm, respectively, significantly blue-shifted compared to commonly obtained blue emitters based on diimine ancillary ligands. The emission profile of complex **3** is identical with those of conceptually analogous blue-emitting isocyanide complexes bearing the same cyclometalating ligands.[54] The difference between the emission spectra of complexes **3** and **4** is that the former exhibits structured emission and the latter shows broad and unstructured emission, pointing to higher ^{3}LC (**3**) and ^{3}MLCT and ^{3}LLCT (**4**) character in the excited states, respectively.[8] In degassed CH_3CN solutions, the PLQYs (0.24 for complex **1** and 0.46 for complex **2**) and excited-state lifetimes (3.3 μs for complex **1** and 6.3 μs for complex **2**) of complexes **1** and **2** are comparable to those of a dfppy-based cationic iridium(III) complex bearing nonconjugated bis-(imidazolium) carbene.[22]

In neat films, the emission maxima of complexes **1** and **2** show a significant red shift with respect to those of the CH_3CN solution, which is related to both self-absorption and strong intermolecular interactions in neat films.[58] These two complexes exhibit low quantum efficiencies compared to those at room temperature because of severe excited-state quenching in neat films. When **1** and **2** were doped (5 wt %) into poly(methyl methacrylate) (PMMA), the PLQYs increase significantly because of suppression of the nonradiative process in the rigid polymer. The PLQYs of complex **1** are lower and vary much more noticeably in CH_3CN solution, PMMA film, and neat film than those of complex **2**, which results from a relatively strong intramolecular stacking interaction preventing large structural relaxations on the excited states. For complex **1**, a relatively weak intramolecular stacking interaction is insufficient to guarantee prevention of this relaxation.[51] In films, we observed a biexponential decay with two components, which means that the different states are not completely equilibrated.[7,59] Complexes **3** and **4** show no emission at room temperature, which can be well explained by their long lifetimes at 77 K in CH_3CN. In neat and doping films, complexes **3** and **4** exhibit short lifetimes compared to those at 77 K. Unfortunately, we failed to obtain the PLQYs of **3** and **4** in dilute CH_3CN solutions and films because of their very weak emission.

Electrochemical Properties. The electrochemical behavior of complexes **1** and **2** was investigated by CV (Figure 3), and the redox potentials versus ferrocenium (Fc^+)/Fc are listed in Table 3. As shown in Figure 3, except for complex **4**, which

dx.doi.org/10.1021/ic5001733 | Inorg. Chem. 2014, 53, 6596−6606

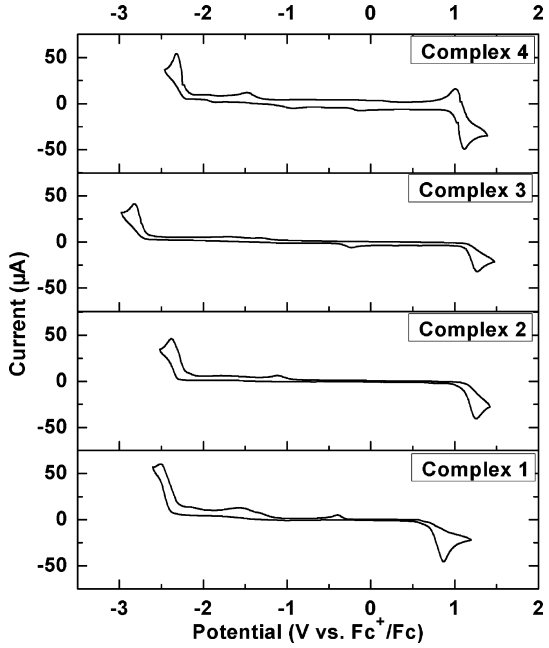

Figure 3. Cyclic voltammograms of complexes **1**–**4** in CH_3CN solutions (2×10^{-3} M). The potentials were recorded versus Fc^+/Fc.

Table 3. Electrochemical Characteristics of Complexes 1–4

complex	E_{ox} (V)	E_{red} (V)	HOMO (eV)[a]	LUMO (eV)[b]	band gap (eV)[c]
1	0.87[d]	−2.50[d]	−5.61	−2.24	3.37
2	1.26[d]	−2.38[d]	−6.00	−2.36	3.64
3	1.27[d]	−2.82[d]	−6.01	−1.92	4.09
4	1.12[e]	−2.32[d]	−5.86	−2.42	3.44

[a]From the formula $E_{HOMO} = -4.74 - eE_{ox}$. [b]From the formula $E_{LUMO} = -4.74 - eE_{red}$. [c]From CV measurements, $E = 1/2(E_{pa} + E_{pc})$; 0.1 M acetonitrile/$TBAPF_6$ versus Fc^+/Fc. [d]An irreversible electrochemical process. [e]A reversible electrochemical process.

presents a reversible oxidation process, other complexes exhibit irreversible reduction and oxidation processes in CH_3CN solutions. The oxidation potentials of complexes **1** (0.87 V), **2** (1.26 V), **3** (1.27 V), and **4** (1.12 V) are similar to those of other ppy-, dfppy-, dfppz-, and dfbpz-based iridium(III) complexes,[7,34,52] respectively. This clearly indicates a similar HOMO localization on the phenyl ring of both the cyclometalated ligands and iridium(III) ions. However, the reduction potentials of complexes **1**–**3** are significantly different from one complex to another despite having identical ancillary ligands. This result points to the LUMOs of **1**–**3** being localized at least partly on the cyclometalated ligand, in contrast to the commonly used cationic iridium(III) complexes, where the LUMO is usually located on the ancillary ligand. The LUMO localization of complex **4** will be discussed in detail by theoretical calculations (see below).

Theoretical Calculations. DFT calculations at the B3LYP/6-31G**+LANL2DZ level were carried out to gain deeper insight into the photophysical and electrochemical properties of complexes **1**–**4** (see the Experimental Section). Electronic ground states of these complexes were directly calculated based on the geometries obtained from their single-crystal structures. Figures 4 and S7–S10 (in the SI) display the composition of the frontier molecular orbitals for complexes **1**–**4**. As expected, the HOMO, HOMO−1, HOMO−2, and HOMO−3 of all complexes are composed of a mixture of Ir d_π orbitals and phenyl π orbitals distributed among the two cyclometalated ligands. Upon attachment of the electron-withdrawing group fluorine to the phenyl ring of cyclometalated ligands, the HOMO level becomes stabilized following the sequence **1** (−7.83 eV), **2** (−8.22 eV), **3** (−8.30 eV), and **4** (−8.30 eV), which is basically in line with the more positive oxidation potentials measured experimentally (**1**, +0.87 V; **2**, +1.26 V; **3**, +1.27 V; **4**, +1.12 V). The LUMO and LUMO+1 of complexes **1** and **2** still reside on the cyclometalated ligands because of their strong stabilization compared with that of nonconjugated ancillary ligand dppmmi. The LUMO, LUMO+1, LUMO+2, and LUMO+3 of complex **3** reside on both the cyclometalated and ancillary ligands because of the higher LUMO energy level of dfppz than those of the ppy and dfppy ligands of complexes **1** and **2**. In contrast to complexes **1**–**3**, the LUMO, LUMO+1, and LUMO+2 of **4** reside almost completely on the ancillary ligand pymbi because of unstabilization of the LUMO of the nonconjugated cyclometalated ligand dfbpz. The reduction potentials of complexes **1**–**4** exhibit no regularity in value because their LUMOs reside on different ligands.

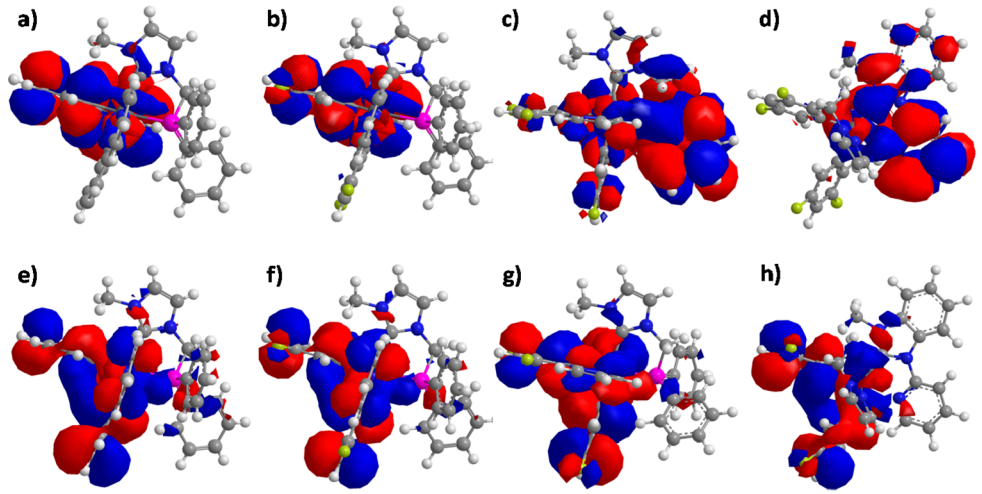

Figure 4. Molecular orbital surfaces of cationic iridium complexes **1**–**4**: (a–d) LUMOs of complexes **1**–**4**; (e–h) HOMOs of complexes **1**–**4**. All of the molecular orbital surfaces correspond to an isocontour value of $|\Psi| = 0.025$.

dx.doi.org/10.1021/ic5001733 | Inorg. Chem. 2014, 53, 6596–6606

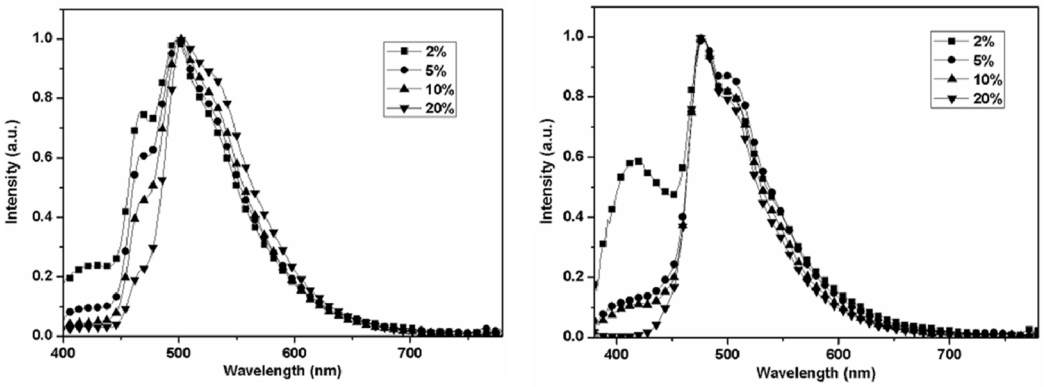

Figure 5. EL spectra of the OLEDs based on complexes **1** (left) and **2** (right) at different doping concentrations (under 8 V).

To further confirm the nature of the emitting excited state, TD-DFT calculations were performed to determine the electronic transition dipole of the low-lying triplet states of complexes **1**–**4**. Table S1 in the SI summarizes the vertical excitation energies and orbitals involved in the excitations for the two calculated lowest triplet states. Two low-lying triplet states (T_1 and T_2) are relatively close in energy and, in principle, emission might occur from any of them.[7,60] TD-DFT calculations predict that T_1 and T_2 show a similar nature for complexes **1** and **2**. It is described as a mixture of MLCT and LC character because the monoelectronic excitations that define T_1 and T_2 involve the HOMO, HOMO−1, HOMO−2, and HOMO−3, which are mixtures of Ir d_π orbitals and ppy (or dfppy) π orbitals, and the LUMO and LUMO+1, which correspond to the cyclometalated ligand. Considering that the photophysical characterization of complexes **1** and **2** agrees with the predominant $^3\pi-\pi^*$ character, we tentatively assign the emission to be predominantly from ppy- and dfppy-based $^3\pi-\pi^*$ states, in contrast to what was found for complexes bearing N^N ancillary ligands.[5,25,29] For complex **3**, T_1 and T_2 have ^{3}MLCT [$d\pi$(Ir) → π^*(dfppz)−π^*(dppmmi)], ^{3}LLCT [π(dfppz) → π^*(dppmmi)], and LC $^3\pi-\pi^*$ [π(dfppz) → π^*(dfppz)] character. In CH_3CN glass at 77 K and neat film, the emission of complex **3** with structured spectra can be assigned to be predominantly from dfppz-based $^3\pi-\pi^*$ states. Complex **4** is the only one that employs nonconjugated dfbpz as the cyclometalated ligand. From the point of view of quantum chemistry, T_1 and T_2 of complex **4** have ^{3}MLCT [$d\pi$(Ir) → π^*(pymbi)] and ^{3}LLCT [π(dfbpz) → π^*(pymbi)] character, which agrees with featureless spectra in CH_3CN glass at 77 K and neat film. This suggests that the emission of complex **4** mainly involves charge transfer from the central iridium(III) ion and cyclometalated ligand to the ancillary ligand with high LUMO energy level, in contrast to commonly designed cationic complexes using carbene-type ancillary ligands,[23,32] where the emission mainly originates from the cyclometalated main ligands. Compared with the low-lying triplet states of complexes **1** and **2** (LC mixed with MLCT), those for both complexes **3** and **4** comprise a substantial LLCT contribution in addition to MLCT and LC. The LC (mixed with MLCT) excited state localized in low-lying triplet states may reduce the radiationless deactivation and therefore increase the PLQYs and stabilities of iridium(III) complexes. Nevertheless, the thermally accessible LLCT transition may cause the associated vibration modes eligible for quenching to increase, which may facilitate radiationless deactivation and, hence, decrease the PLQYs.[55] This can be responsible for the high PLQYs of complexes **1** and **2** and very weak emission of complexes **3** and **4** in dilute CH_3CN solutions and films.

EL Properties. In order to evaluate the EL properties of blue-emitting complexes **1** and **2**, we fabricated the OLEDs and employed them as doped emitters by the solution process. The device structure is ITO/(PEDOT:PSS) (40 nm)/PVK:OXD-7:*x*% complex **1** (or **2**) (80 nm)/TPBI (30 nm)/Cs_2CO_3 (4 nm)/Al (120 nm). PEDOT:PSS acts as a hole-injecting layer. To facilitate electron transport in the light-emitting layers, OXD-7 is mixed into PVK as the cohost. TPBI acts as both an exciton blocker and electron transporter and Cs_2CO_3/Al as the electron-injection layer and cathode. For optimization purposes, the doping level of each iridium phosphor was varied at four different weight concentrations (*x*% = 2%, 5%, 10%, and 20%, respectively).

EL spectra of the OLEDs based on complexes **1** and **2** at different doping concentrations (under 8 V) are depicted in Figure 5, and detailed electrical characteristics are summarized in Table 4. Devices based on complex **1** as the dopant show blue-green-light emission with the emission peak at about 498 nm accompanied by two shoulder peaks at 466 and 517 nm, respectively. The Commission International de L'Eclairage (CIE) color coordinates of the four devices vary from (0.22, 0.38) to (0.28, 0.54), and the turn-on voltages ($V_{turn\text{-}on}$) are about 5.3–7.2 V. Devices based on complex **2** exhibit blue-light

Table 4. Electrical Characteristics of Devices Based on Complexes 1 and 2

phosphor dopant	$V_{turn\text{-}on}$/V	L_{max} /cd m^{-2} (V^a)	η_L /cd A^{-1} (V^a)	λ_{em}/ nm	CIE (*x*, *y*)
1 (2 wt %)	5.3	1046 (13.0)	3.1 (5.9)	498	(0.22, 0.38)
1 (5 wt %)	6.1	1228 (13.0)	3.3 (8.0)	498	(0.24, 0.43)
1 (10 wt %)	6.0	1125 (13.0)	3.8 (8.2)	498	(0.24, 0.48)
1 (20 wt %)	7.2	1552 (17.0)	2.4 (10.9)	498	(0.28, 0.54)
2 (2 wt %)	5.3	651 (14.2)	1.3 (7.6)	478	(0.21, 0.30)
2 (5 wt %)	5.8	602 (13.0)	1.4 (7.6)	478	(0.21, 0.38)
2 (10 wt %)	5.8	986 (14.0)	3.0 (6.6)	478	(0.20, 0.38)
2 (20 wt %)	6.2	730 (15.0)	3.4 (9.2)	478	(0.20, 0.38)

[a]Maximum values of the devices. Values in parentheses are the voltages at which they were obtained.

dx.doi.org/10.1021/ic5001733 | Inorg. Chem. 2014, 53, 6596–6606

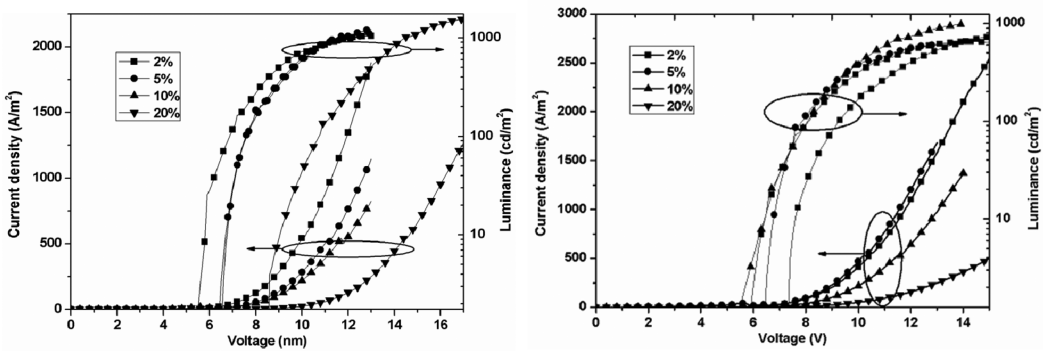

Figure 6. Luminance−voltage−current density characteristics of the OLEDs based on complexes **1** (left) and **2** (right) at different doping levels.

emission with the emission peak at about 478 nm and a shoulder peak at 501 nm. The CIE color coordinates of the four devices vary a little from (0.20, 0.38) to (0.21, 0.30), which present much blue-shift with respect to electrophosphorescence based on complex **1**. However, at low doping concentrations of the dopant (2% and 5% for complex **1** and 2%, 5%, and 10% for complex **2**), a weak emission (417 nm) from PVK:OXD-7 was observed, indicating incomplete energy transfer from PVK:OXD-7 to complexes **1** and **2**. With an increase of the doping concentration to 20%, emission from PVK:OXD-7 disappeared. The emission wavelengths of EL spectra of complexes **1** and **2** closely resemble those of the PL spectra in solutions or thin films, indicating that electroluminescence originated from the doped cationic iridium complexes **1** and **2**.

Figure 6 shows the luminance−voltage−current density characteristics of devices with different doping concentrations of complexes **1** and **2**. As depicted in Figure 6, the best performances of the devices are achieved at the doping level of 10 wt % for complex **1** and 20 wt % for complex **2**. For complex **1**, a maximum luminance (L_{max}) of 1552 cd m^{-2} at 17 V and a maximum luminance efficiency (η_L) of 3.8 cd A^{-1} at 8.2 V are achieved. For complex **2**, a maximum luminance (L_{max}) of 986 cd m^{-2} at 14 V and a maximum luminance efficiency (η_L) of 3.4 cd A^{-1} at 9.2 V are achieved. The devices based on complexes **1** and **2** exhibit inferior EL properties compared with those of other cationic iridium(III) complexes.[14,16,21] The relatively low efficiency and brightness of these devices are presumably due to the relatively low triplet energy of the PVK host[61,62] or the inefficient energy transfer from the PVK:OXD-7 host to these complexes (vide supra). Further work is to dope complexes **1** and **2** into a host with higher triplet energy to improve the efficiency of the blue device.

CONCLUSION

We have prepared two series of cationic iridium(III) complexes **1**−**4** with nonconjugated ancillary and cyclometalating ligands, respectively. Nonconjugated ligands are introduced in this work in order to restrict the electronic transition dipole of the emitting triplet state mainly around the chromophoric ligands with high LUMO energy levels. This conceptual design is further supported by the corresponding photophysical characterization, electrochemical properties, and computational approaches in this study. The result revealed that the electronic transition dipole of cationic iridium complexes could be mainly confined to cyclometalated ligands (^{3}MLCT and LC $^3\pi-\pi^*$) when a nonconjugated ancillary ligand is used and to the central iridium(III) ion and cyclometalated ligand to ancillary ligand charge transfer (^{3}MLCT and ^{3}LLCT) when non-conjugated cyclometalated ligands are used. As anticipated, short-wavelength light emission can be achieved through the use of a chromophoric ligand with high LUMO energy level based on a facile synthetic approach. Solution-processed OLEDs based on complexes **1** and **2** gave blue-green (498 nm) and blue (478 nm) electroluminescence with maximum current efficiencies of 3.8 and 3.4 cd A^{-1}, respectively. This work provides guidelines for developing efficient blue-charged phosphorescent complexes used in organic EL devices.

ASSOCIATED CONTENT

Supporting Information

Synthesis, NMR and ESI-MS spectra, selected triplet states, listings of distributions of selected molecular orbitals, and CIF files of complexes **1**−**4**. This material is available free of charge via the Internet at http://pubs.acs.org.

AUTHOR INFORMATION

Corresponding Authors

*E-mail: zhangfuli@sqnc.edu.cn. Phone: 86-370-2592844.
*E-mail: duanl@mail.tsinghua.edu.cn. Phone: 86-10-62782287.

Notes

The authors declare no competing financial interest.

ACKNOWLEDGMENTS

We thank the National Natural Science Foundation of China (Grants 51173096, 21161160447, and 61177023) for financial support. In addition, we thank Prof. Taiju Tsuboi of Nanjing University of Technology and Prof. Yun Chi of National Tsing Hua University (Hsinchu) for valuable suggestions on the photophysical properties of the complexes.

REFERENCES

(1) Slinker, J. D.; Gorodetsky, A. A.; Lowry, M. S.; Wang, J. J.; Parker, S.; Rohl, R.; Bernhard, S.; Malliaras, G. G. *J. Am. Chem. Soc.* **2004**, *126*, 2763−2767.
(2) Su, H. C.; Chen, H. F.; Wu, C. C.; Wong, K. T. *Chem.—Asian J.* **2008**, *3*, 1922−1928.
(3) Bolink, H. J.; Coronado, E.; Costa, R. D.; Orti, E.; Sessolo, M.; Graber, S.; Doyle, K.; Neuburger, M.; Housecroft, C. E.; Constable, E. C. *Adv. Mater.* **2008**, *20*, 3910−3913.
(4) Costa, R. D.; Orti, E.; Bolink, H. J.; Graber, S.; Housecroft, C. E.; Constable, E. C. *Chem. Commun.* **2011**, *47*, 3207−3209.
(5) Costa, R. D.; Orti, E.; Bolink, H. J.; Graber, S.; Schaffner, S.; Neuburger, M.; Housecroft, C. E.; Constable, E. C. *Adv. Funct. Mater.* **2009**, *19*, 3456−3463.
(6) Margapoti, E.; Shukla, V.; Valore, A.; Sharma, A.; Dragonetti, C.; Kitts, C. C.; Roberto, D.; Murgia, M.; Ugo, R.; Muccini, M. *J. Phys. Chem. C* **2009**, *113*, 12517−12522.

(7) He, L.; Duan, L.; Qiao, J.; Wang, R. J.; Wei, P.; Wang, L. D.; Qiu, Y. *Adv. Funct. Mater.* **2008**, *18*, 2123−2131.
(8) He, L.; Qiao, J.; Duan, L.; Dong, G. F.; Zhang, D. Q.; Wang, L. D.; Qiu, Y. *Adv. Funct. Mater.* **2009**, *19*, 2950−2960.
(9) Orselli, E.; Albuquerque, R. Q.; Fransen, P. M.; Frohlich, R.; Janssen, H. M.; De Cola, L. *J. Mater. Chem.* **2008**, *18*, 4579−4590.
(10) Su, H. C.; Chen, H. F.; Fang, F. C.; Liu, C. C.; Wu, C. C.; Wong, K. T.; Liu, Y. H.; Peng, S. M. *J. Am. Chem. Soc.* **2008**, *130*, 3413−3419.
(11) Zhang, F. L.; Duan, L.; Qiao, J.; Dong, G. F.; Wang, L. D.; Qiu, Y. *Org. Electron.* **2012**, *13*, 2442−2449.
(12) Mydlak, M.; Bizzarri, C.; Hartmann, D.; Sarfert, W.; Schmid, G.; De Cola, L. *Adv. Funct. Mater.* **2010**, *20*, 1812−1820.
(13) Costa, R. D.; Orti, E.; Bolink, H. J.; Monti, F.; Accorsi, G.; Armaroli, N. *Angew. Chem., Int. Ed.* **2012**, *51*, 8178−8211.
(14) Plummer, E. A.; van Dijken, A.; Hofstraat, H. W.; De Cola, L.; Brunner, K. *Adv. Funct. Mater.* **2005**, *15*, 281−289.
(15) Wong, W. Y.; Zhou, G. J.; Yu, X. M.; Kwok, H. S.; Lin, Z. Y. *Adv. Funct. Mater.* **2007**, *17*, 315−323.
(16) He, L.; Duan, L.; Qiao, J.; Zhang, D. Q.; Dong, G. F.; Wang, L. D.; Qiu, Y. *Org. Electron.* **2009**, *10*, 152−157.
(17) He, L.; Duan, L. A.; Qiao, J. A.; Zhang, D. Q.; Wang, L. D.; Qiu, Y. *Org. Electron.* **2010**, *11*, 1185−1191.
(18) Fernandez-Hernandez, J. M.; Yang, C. H.; Beltran, J. I.; Lemaur, V.; Polo, F.; Frohlich, R.; Cornil, J.; De Cola, L. *J. Am. Chem. Soc.* **2011**, *133*, 10543−10558.
(19) Tao, R.; Qiao, J.; Zhang, G. L.; Duan, L.; Wang, L. D.; Qiu, Y. *J. Phys. Chem. C* **2012**, *116*, 11658−11664.
(20) Zhang, F. L.; Duan, L.; Qiao, J.; Dong, G. F.; Wang, L. D.; Qiu, Y. *Org. Electron.* **2012**, *13*, 1277−1288.
(21) Tang, H. J.; Li, Y. H.; Zhao, B. F.; Yang, W.; Wu, H. B.; Cao, Y. *Org. Electron.* **2012**, *13*, 3211−3219.
(22) Yang, C. H.; Beltran, J.; Lemaur, V.; Cornil, J.; Hartmann, D.; Sarfert, W.; Frohlich, R.; Bizzarri, C.; De Cola, L. *Inorg. Chem.* **2010**, *49*, 9891−9901.
(23) Kessler, F.; Costa, R. D.; Di Censo, D.; Scopelliti, R.; Orti, E.; Bolink, H. J.; Meier, S.; Sarfert, W.; Gratzel, M.; Nazeeruddin, M. K.; Baranoff, E. *Dalton Trans.* **2012**, *41*, 180−191.
(24) Meier, S. B.; Sarfert, W.; Junquera-Hernandez, J. M.; Delgado, M.; Tordera, D.; Orti, E.; Bolink, H. J.; Kessler, F.; Scopelliti, R.; Gratzel, M.; Nazeeruddin, M. K.; Baranoff, E. *J. Mater. Chem. C* **2013**, *1*, 58−68.
(25) Tamayo, A. B.; Garon, S.; Sajoto, T.; Djurovich, P. I.; Tsyba, I. M.; Bau, R.; Thompson, M. E. *Inorg. Chem.* **2005**, *44*, 8723−8732.
(26) Lowry, M. S.; Hudson, W. R.; Pascal, R. A.; Bernhard, S. *J. Am. Chem. Soc.* **2004**, *126*, 14129−14135.
(27) Lowry, M. S.; Goldsmith, J. I.; Slinker, J. D.; Rohl, R.; Pascal, R. A.; Malliaras, G. G.; Bernhard, S. *Chem. Mater.* **2005**, *17*, 5712−5719.
(28) Nazeeruddin, M. K.; Wegh, R. T.; Zhou, Z.; Klein, C.; Wang, Q.; De Angelis, F.; Fantacci, S.; Gratzel, M. *Inorg. Chem.* **2006**, *45*, 9245−9250.
(29) De Angelis, F.; Fantacci, S.; Evans, N.; Klein, C.; Zakeeruddin, S. M.; Moser, J. E.; Kalyanasundaram, K.; Bolink, H. J.; Gratzel, M.; Nazeeruddin, M. K. *Inorg. Chem.* **2007**, *46*, 5989−6001.
(30) Chen, B.; Li, Y. H.; Yang, W.; Luo, W.; Wu, H. B. *Org. Electron.* **2011**, *12*, 766−773.
(31) Chi, Y.; Chou, P. T. *Chem. Soc. Rev.* **2010**, *39*, 638−655.
(32) Monti, F.; Kessler, F.; Delgado, M.; Frey, J.; Bazzanini, F.; Accorsi, G.; Armaroli, N.; Bolink, H. J.; Ortí, E.; Scopelliti, R.; Nazeeruddin, M. K.; Baranoff, E. *Inorg. Chem.* **2013**, *52*, 10292−10305.
(33) Darmawan, N.; Yang, C. H.; Mauro, M.; Raynal, M.; Heun, S.; Pan, J.; Buchholz, H.; Braunstein, P.; De Cola, L. *Inorg. Chem.* **2013**, *52*, 10756−10765.
(34) Song, Y. H.; Chiu, Y. C.; Chi, Y.; Cheng, Y. M.; Lai, C. H.; Chou, P. T.; Wong, K. T.; Tsai, M. H.; Wu, C. C. *Chem.—Eur. J.* **2008**, *14*, 5423−5434.
(35) Chiu, Y. C.; Hung, J. Y.; Chi, Y.; Chen, C. C.; Chang, C. H.; Wu, C. C.; Cheng, Y. M.; Yu, Y. C.; Lee, G. H.; Chou, P. T. *Adv. Mater.* **2009**, *21*, 2221−2225.
(36) Chiu, Y. C.; Chi, Y.; Hung, J. Y.; Cheng, Y. M.; Yu, Y. C.; Chung, M. W.; Lee, G. H.; Chou, P. T.; Chen, C. C.; Wu, C. C.; Hsieh, H. Y. *ACS Appl. Mater. Interfaces* **2009**, *1*, 433−442.
(37) Chang, C. F.; Cheng, Y. M.; Chi, Y.; Chiu, Y. C.; Lin, C. C.; Lee, G. H.; Chou, P. T.; Chen, C. C.; Chang, C. H.; Wu, C. C. *Angew. Chem., Int. Ed.* **2008**, *47*, 4542−4545.
(38) Meng, S.; Jung, I.; Feng, J.; Scopelliti, R.; Di Censo, D.; Grätzel, M.; Nazeeruddin, M. K.; Baranoff, E. *Eur. J. Inorg. Chem.* **2012**, *2012*, 3209−3215.
(39) Song, G. Y.; Li, X. W.; Song, Z. C.; Zhao, J.; Zhang, H. J. *Chem.—Eur. J.* **2009**, *15*, 5535−5544.
(40) Chianese, A. R.; Bremer, P. T.; Wong, C.; Reynes, R. J. *Organometallics* **2009**, *28*, 5244−5252.
(41) Nonoyama, M. *Bull. Chem. Soc. Jpn.* **1974**, *47*, 767−768.
(42) Melhuish, W. H. *J. Phys. Chem.* **1961**, *65*, 229−235.
(43) Pålsson, L. O.; Monkman, A. P. *Adv. Mater.* **2002**, *14*, 757−758.
(44) Sheldrick, G. M. *Acta Crystallogr.* **2008**, *A64*, 112−122.
(45) Becke, A. D. *J. Chem. Phys.* **1993**, *98*, 5648−5652.
(46) Lee, C. T.; Yang, W. T.; Parr, R. G. *Phys. Rev. B* **1988**, *37*, 785−789.
(47) Francl, M. M.; Pietro, W. J.; Hehre, W. J.; Binkley, J. S.; Gordon, M. S.; Defrees, D. J.; Pople, J. A. *J. Chem. Phys.* **1982**, *77*, 3654−3665.
(48) Hay, P. J.; Wadt, W. R. *J. Chem. Phys.* **1985**, *82*, 299−310.
(49) Frisch, M. J.; Trucks, G. W.; Schlegel, H. B.; Scuseria, G. E.; Robb, M. A.; Cheeseman, J. R.; Montgomery, J., Jr.; Vreven, T.; Kudin, K. N.; Burant, J. C.; Millam, J. M.; Iyengar, S. S.; Tomasi, J.; Barone, V.; Mennucci, B.; Cossi, M.; Scalmani, G.; Rega, N.; Petersson, G. A.; Nakatsuji, H.; Hada, M.; Ehara, M.; Toyota, K.; Fukuda, R.; Hasegawa, J.; Ishida, M.; Nakajima, T.; Honda, Y.; Kitao, O.; Nakai, H.; Klene, M.; Li, X.; Knox, J. E.; Hratchian, H. P.; Cross, J. B.; Bakken, V.; Adamo, C.; Jaramillo, J.; Gomperts, R.; Stratmann, R. E.; Yazyev, O.; Austin, A. J.; Cammi, R.; Pomelli, C.; Ochterski, J. W.; Ayala, P. Y.; Morokuma, K.; Voth, G. A.; Salvador, P.; Dannenberg, J. J.; Zakrzewski, V. G.; Dapprich, S.; Daniels, A. D.; Strain, M. C.; Farkas, O.; Malick, D. K.; Rabuck, A. D.; Raghavachari, K.; Foresman, J. B.; Ortiz, J. V.; Cui, Q.; Baboul, A. G.; Clifford, S.; Cioslowski, J.; Stefanov, B. B.; Liu, G.; Liashenko, A.; Piskorz, P.; Komaromi, I.; Martin, R. L.; Fox, D. J.; Keith, T.; Al-Laham, M. A.; Peng, C. Y.; Nanayakkara, A.; Challacombe, M.; Gill, P. M. W.; Johnson, B.; Chen, W.; Wong, M. W.; Gonzalez, C.; Pople, J. A. *Gaussian 03*, revision B.05; Gaussian, Inc.: Wallingford, CT, 2004.
(50) He, L.; Duan, L.; Qiao, J.; Zhang, D.; Wang, L.; Qiu, Y. *Chem. Commun.* **2011**, *47*, 6467−6469.
(51) He, L.; Ma, D.; Duan, L.; Wei, Y.; Qiao, J.; Zhang, D.; Dong, G.; Wang, L.; Qiu, Y. *Inorg. Chem.* **2012**, *51*, 4502−4510.
(52) He, L.; Duan, L.; Qiao, J.; Dong, G. F.; Wang, L. D.; Qiu, Y. *Chem. Mater.* **2010**, *22*, 3535−3542.
(53) Sajoto, T.; Djurovich, P. I.; Tamayo, A.; Yousufuddin, M.; Bau, R.; Thompson, M. E.; Holmes, R. J.; Forrest, S. R. *Inorg. Chem.* **2005**, *44*, 7992−8003.
(54) Shavaleev, N. M.; Monti, F.; Scopelliti, R.; Baschieri, A.; Sambri, L.; Armaroli, N.; Grätzel, M.; Nazeeruddin, M. K. *Organometallics* **2013**, *32*, 460−467.
(55) Fu, H.; Cheng, Y.-M.; Chou, P.-T.; Chi, Y. *Mater. Today* **2011**, *14*, 472−479.
(56) Colombo, M. G.; Gudel, H. U. *Inorg. Chem.* **1993**, *32*, 3081−3087.
(57) Colombo, M. G.; Hauser, A.; Gudel, H. U. *Inorg. Chem.* **1993**, *32*, 3088−3092.
(58) Clementi, C.; Miliani, C.; Verri, G.; Sotiropoulou, S.; Romani, A.; Brunetti, B. G.; Sgamellotti, A. *Appl. Spectrosc.* **2009**, *63*, 1323−1330.
(59) Ramachandra, S.; Polo, F.; Edafe, F.; Schuermann, K. C.; Nijhuis, C. A.; Belser, P.; Reus, W. F.; Whitesides, G. M.; De Cola, L. *Pure Appl. Chem.* **2011**, *83*, 779−799.
(60) Bolink, H. J.; Cappelli, L.; Cheylan, S.; Coronado, E.; Costa, R. D.; Lardiés, N.; Nazeeruddin, M. K.; Ortí, E. *J. Mater. Chem.* **2007**, *17*, 5032.

(61) Yokoyama, M.; Tamamura, T.; Nakano, T.; Mikawa, H. *J. Chem. Phys.* **1976**, *65*, 272−279.
(62) Rippen, G.; Kaufmann, G.; Klopffer, W. *Chem. Phys.* **1980**, *52*, 165−177.